

Site-selective ion production of the core-excited CH₃F molecule probed by Auger-electron-ion coincidence measurements

X. J. Liu,¹ G. Prümper,¹ E. Kukk,^{1,2} R. Sankari,³ M. Hoshino,⁴ C. Makochekanwa,^{5,6} M. Kitajima,⁵ H. Tanaka,⁵ H. Yoshida,⁷ Y. Tamenori,⁸ and K. Ueda^{1,*}

¹*Institute of Multidisciplinary Research for Advanced Materials, Tohoku University, Sendai 980-8577, Japan*

²*Department of Physics, Materials Science, University of Turku, Finland*

³*Department of Physics Science, University of Oulu, Oulu, Finland*

⁴*Atomic Physics Laboratory, RIKEN, Wako, Saitama 351-0198, Japan*

⁵*Department of Physics, Sophia University, Tokyo 102-8554, Japan*

⁶*Graduate School of Sciences, Kyushu University, Fukuoka 812-8581, Japan*

⁷*Department of Chemistry, Hiroshima University, Higashi-Hiroshima, Japan*

⁸*Japan Synchrotron Radiation Research Institute, Sayo-gun, Hyogo, Japan*

(Received 11 April 2005; published 11 October 2005)

We have carried out a coincidence experiment between energy-resolved resonant Auger electrons and mass-resolved ions on CH₃F molecules following F 1s and C 1s excitation to the lowest unoccupied C–F antibonding molecular orbital σ_{CF}^* . We found a strong enhancement of the F⁺ or CH⁺ ion production in coincidence with the F KVV and C KVV spectator Auger electrons, respectively, in the wide binding energy range of 28–36 eV. This site-selective ion production is interpreted as a consequence of the resonant Auger emission taking place in the transient region where the C–F elongation caused by the core excitation transforms the molecular valence orbitals gradually into nonoverlapping valence orbitals of each fragment.

DOI: [10.1103/PhysRevA.72.042704](https://doi.org/10.1103/PhysRevA.72.042704)

PACS number(s): 32.80.Hd, 33.80.Eh, 33.80.Gj

I. INTRODUCTION

To study molecular photodissociation in detail, it is highly advantageous to employ site-specific core excitation [1]. Benefits of this technique lie in the clear characterization of the initial state, where the energy, symmetry, and lifetime are known. One of the most exciting findings in the dissociation of core-excited molecules is site-specific fragmentation. Bond breaking often takes place near the excited atomic site, as demonstrated by Eberhardt *et al.*: they found that only O ions are produced when the C 1s electron in the CO site in a (CH₃)₂CO molecule is excited to the lowest unoccupied molecular orbital (LUMO) π^* [2]. Between the site-specific core excitation and the ionic fragmentation, however, there is one more step: the system undergoes Auger decay and the energies of its final states may be widely spread and each final state with different energy may result in a different ionic fragmentation pathway. Thus a coincidence experiment between the energy-resolved Auger electron and the fragment ion is demanded in order to specify a dissociation pathway [3–5] and to investigate the mechanism leading to the site-specific fragmentation [6,7]. Core-excited states of molecules have an equilibrium geometry different from that of the neutral ground state and thus nuclear motion is caused by photoexcitation, leading to molecular deformation. The molecular deformation may open up new site-specific dissociation channels. The question of whether the nuclear motion and deformation caused by core excitation plays any role can be answered by the Auger-electron-ion coincidence measure-

ment. Indeed, Morin and co-workers [8,9] successfully investigated the influence of the nuclear motion in the core-excited state to the molecular dissociation, using the resonant Auger electron-ion coincidence technique. There are two classes of resonant Auger decay, participator Auger decay and spectator Auger decay. In the participator decay, the electron promoted from the core orbital to the unoccupied molecular orbital participates in the decay and thus its final state can be denoted as V^{-1} . In the spectator decay, the promoted electron stays as a spectator during the decay and thus its final state can be denoted as V^{-2} plus one spectator electron. In their investigations, Morin and co-workers focused on the participator Auger decay and found evidence that the nuclear relaxation caused in the core-excited state affects the vibrational distribution in a Auger final state V^{-1} , which in turn leads to a specific molecular dissociation channel.

In this paper, we present a showcase example for site-specific fragmentation, i.e., the site-selective ion production from the core-excited CH₃F molecule, to demonstrate that the nuclear relaxation caused in the F or C 1s core-excited state plays a key role in switching the ion production. The CH₃F molecule in the ground state has a geometrical symmetry of C_{3v} and its electronic configuration is written as

$$1a_1^2 2a_1^2 3a_1^2 4a_1^2 1e^4 5a_1^2 2e^4 X^1A_1.$$

Here $1a_1$ and $2a_1$ correspond to the F and C K-shell orbitals, respectively. The lowest unoccupied molecular orbital (LUMO) $6a_1$ has a C–F antibonding character and is often designated as σ_{CF}^* . Because of this antibonding nature, a C–F stretching motion is caused by a promotion of $1a_1 \rightarrow 6a_1$ or $2a_1 \rightarrow 6a_1$ via photoexcitation. The lifetime is ~ 3 fs for the F 1s-hole state [10] and ~ 7 fs for the C 1s-hole state

*Corresponding author. Electronic address: ueda@tagen.tohoku.ac.jp

[11,12]. The system undergoes the so-called *KVV* resonant Auger decay in this time scale, in competition with elongation of the C–F bond. In the present work, we focus on the spectator Auger final states with two valence holes V^{-2} and one electron in $6a_1$, instead of the participator Auger final state V^{-1} , because spectator Auger final states with a $6a_1$ electron are expected to be dissociative along the C–F bond, and to lead to site-specific ionic fragmentation. To specify the *KVV* Auger final states $V^{-2}6a_1$, we use the Auger electron-ion coincidence technique [13–15].

II. EXPERIMENT

The experiments were conducted at the *c* branch of the Soft X-ray Photochemistry Beamline 27SU [16] at SPring-8, the 8-GeV synchrotron radiation facility in Japan. The monochromator installed in this beam line is of Hettrick type and a resolution of over 10 000 can be achieved [17]. The light source is a figure-8 undulator [18]. With this undulator, one can switch the direction of polarization between horizontal (using first-order harmonic) and vertical (using the so-called 0.5th-order harmonic), by only adjusting the gap of the undulator. In the present experiment, we employed the horizontal polarization.

The experimental setup and the data acquisition system are described in detail in Refs. [13,14]. Briefly, the setup consists of a hemispherical electron spectrometer (SES-2002) and an ion time-of-flight (TOF) spectrometer mounted inside a vacuum chamber. The sample gas CH_3F is introduced between the pusher and extractor electrodes of the ion spectrometer through a grounded copper needle. Electrons pass the pusher electrode and enter the electron spectrometer equipped with a delay-line detector (Roentdek DLD40). During the coincidence experiment, all voltages of the electron spectrometer were fixed. Triggered by the electron detection, rectangular high voltage pulses with opposite signs are generated by a pulse generator (GPTA HVC-1000) and applied to the pusher and extractor electrodes. The ions are detected by another delay-line detector with an active diameter of 80 mm (Roentdek DLD80) set at the end of the TOF drift tube. All data are recorded by multichannel time to digital converters (TDC) (Roentdek TDC-8) and stored in the list mode for off-line analysis. The contribution from the random coincidences has been subtracted, using the procedure described elsewhere [13].

III. RESULTS

Figures 1(a) and 1(b) present the electron spectra of CH_3F at photon energies 687.8 and 288.8 eV, respectively. These spectra were recorded as references, without taking coincidence with ions, using a gas cell, instead of the molecular beam, and a charge-coupled device camera instead of the delayline detector. The overall resolutions were ~ 0.2 eV for both spectra. These photon energies correspond to a promotion of the F 1s ($1a_1$) and C 1s ($2a_1$) electron, respectively, to the σ_{CF}^* ($6a_1$) orbital. The electron emission was detected in the direction parallel to the light polarization vector. The binding energies of the valence orbitals are 13.1 eV ($2e$),

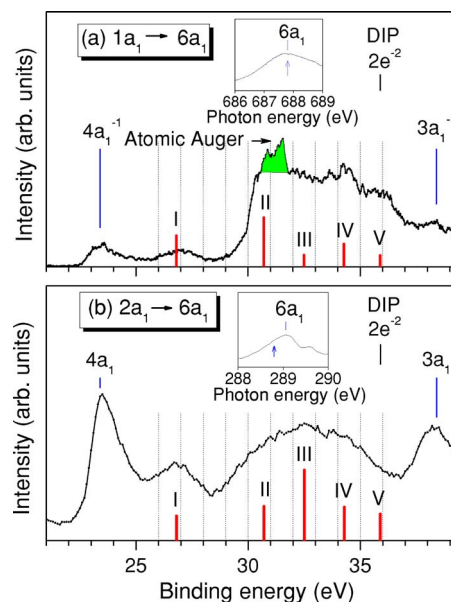


FIG. 1. (Color online) Resonant Auger electron spectra, recorded at photon energies tuned to (a) $1a_1$ (F 1s) $\rightarrow 6a_1$ at 687.8 eV and (b) $2a_1$ (C 1s) $\rightarrow 6a_1$ for CH_3F at 288.8 eV. The insets show photoabsorption spectra, in which the arrows indicate the photon energies where the resonant Auger electron spectra, as well as the electron-ion coincidence spectra are measured. The measurements were along the direction of the light polarization. The Roman numbers I, II, III, IV, and V represent the spectator Auger lines $2e^{-2}6a_1$, $5a_1^{-1}2e^{-1}6a_1$, $1e^{-1}2e^{-1}6a_1$, $5a_1^{-1}1e^{-1}$, and $5a_1^{-2}6a_1$, respectively. The height of each vertical bar reflects the intensity of the corresponding normal Auger transition calculated by Ref. [22].

17.2 eV ($5a_1$ and $1e$), 23.4 eV ($4a_1$), and 38.4 eV ($3a_1$) [19–21]. The range of the binding energy, or the ionization potential, shown in Fig. 1, thus corresponds to the low energy part of the spectator Auger final states $V^{-2}6a_1$ located between the two participator Auger lines at 23.4 eV ($4a_1$) and 38.4 eV ($3a_1$). Though no calculations are available for the resonant Auger spectra, the *IP*s for the spectator Auger final states $V^{-2}6a_1$ can be roughly estimated from the double ionization potentials *DIP* of the normal Auger final two-hole states V^{-2} , taking into account the binding energy $B(6a_1)$ of the additional spectator electron $6a_1$:

$$IP = DIP - B(6a_1) \quad (1)$$

The values of *DIP* are taken from Liegener [22] and $B(6a_1)$ is chosen to be 9.1 eV, to obtain the best overall agreement with the experimental spectra shown in Fig. 1. The *IP*s of the states $2e^{-2}6a_1$, $2e^{-1}5a_1^{-1}6a_1$, $2e^{-1}1e^{-1}6a_1$, $5a_1^{-1}1e^{-1}6a_1$, and $5a_1^{-2}6a_1$ thus obtained are indicated in Fig. 1 by the vertical bars labeled with Roman numbers I–V. The height of each vertical bar reflects the intensity of the corresponding Auger transition calculated by Ref. [22]. Although the model employed here is rather crude, the general agreement is fair. The weak lowest energy peak at $IP \sim 27$ eV can be assigned to $2e^{-2}6a_1$. Other electronic states $V^{-2}6a_1$ are not well resolved for either of the F 1s or C 1s spectator decay spectra. It should be noted that, in the above calculations, the nuclei

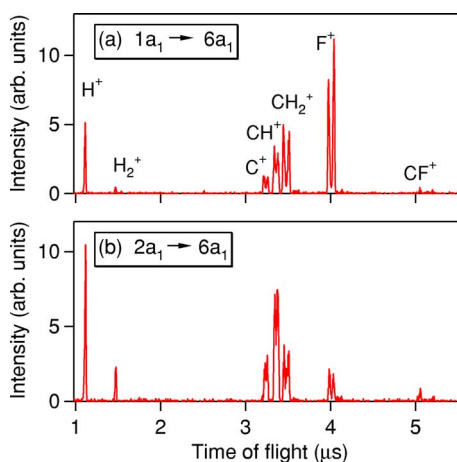


FIG. 2. (Color online) TOF spectra coincident with (a) F *KVV* and (b) C *KVV* spectator Auger electrons, with binding energy between 30 and 31 eV. The area of the entire range of the TOF spectrum is normalized to be the same.

were fixed to the ground-state stable geometry and the nuclear relaxation was neglected.

We show the ion TOF spectra recorded in coincidence with F *KVV* and C *KVV* resonant Auger electrons in the binding energy 30–31 eV in Figs. 2(a) and 2(b), respectively. The TOF spectra were normalized by scaling the total area of the TOF spectrum to 1. Each TOF peak of CH_n^+ and F^+ has a double-peak structure. This indicates that the C–F bond breaking takes place preferentially along the *E* vector that coincides with the TOF axis. The ion ejected in the direction of the ion detector arrives earlier than an ion at rest, while the ion ejected in the opposite direction turns around in the applied electric field and arrives later. As a result, each TOF peak splits into two components representing early and late arrivals of the ions. It is also worth to note that there are almost no CH_3^+ or CH_nF^+ ions ($n=0, \dots, 3$) in the spectra.

We have extracted the ratios of the ion production from the ion TOF spectra, similar to the ones in Fig. 2, recorded in coincidence with the spectator Auger electrons, with the selected binding energies with a 1-eV bandwidth in the region 26–36 eV, which includes spectator Auger final states $2e^{-2}6a_1$, $2e^{-15}a_1^{-1}6a_1$, $2e^{-11}e^{-1}6a_1$, $5a_1^{-1}e^{-1}6a_1$, and $5a_1^{-2}6a_1$. In Fig. 3, we present the results of the relative contributions thus obtained. The relative contribution of H^+ increases, while that of CH_2^+ decreases, as the binding energy increases. This may be a natural consequence of a more complete fragmentation of the molecule taking place for higher energy states. The key finding of this experiment, however, is derived from the comparison of the ion production ratios for the F $1s$ ($1a_1$) and C $1s$ ($2a_1$) promotions shown in Figs. 3(a) and 3(b), respectively. We notice that the ion contributions are relatively similar for the binding energy region 26–28 eV and that they are significantly different in the regions 28–34 eV. The most striking difference can be found in the region 30–32 eV, where F^+ is dominant for the F $1s$ ($1a_1$) promotion and CH^+ is dominant for the C $1s$ ($2a_1$) promotion.

IV. DISCUSSION

We first assume that the nuclear relaxation is negligible within the core-hole lifetime and the resonant Auger decay

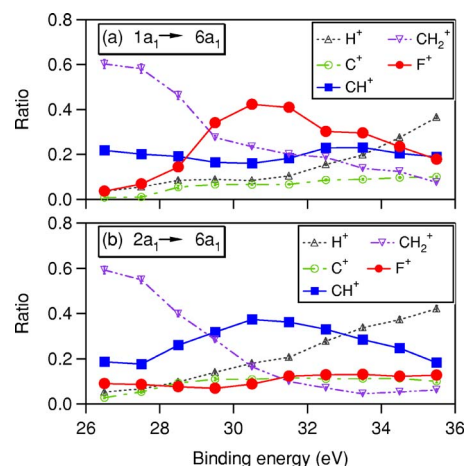


FIG. 3. (Color online) Ion production ratios with (a) F *KVV* and (b) C *KVV* spectator Auger electrons, as a function of the binding energy of the Auger final states. The statistical uncertainties (1σ) are within the size of the data points, or represented by short vertical lines if they are larger than the marks.

takes place within the Franck-Condon region defined by the zero-point vibrational wave function of the ground state. Then the distribution of ionic fragments from the electronic state $V^{-2}6a_1$ populated via C *KVV* spectator Auger decay should be identical to the distribution resulting from $V^{-2}6a_1$ populated via F *KVV* spectator Auger decay. For the lowest-energy band at ~ 27 eV, which is likely to be assigned to $2e^{-2}6a_1$, the above prediction seems to work. However, this prediction sharply contradicts with the present observation in the binding energy region 28–34 eV, as seen in Fig. 3.

Now we discuss the effect of the nuclear relaxation in the core-excited state in which F $1s$ ($1a_1$) or C $1s$ ($2a_1$) is promoted to $\sigma_{\text{CF}}^*(6a_1)$ via photoexcitation. For this core-excited state the nuclear relaxation is expected to be a C–F stretching motion because of the strong antibonding nature of the $6a_1$ orbital. Let us consider the asymptotic case, where the C–F bond breaking takes place first and then electronic decay occurs in the fragment. Here the bond breaking means that there are no longer valence orbitals overlapping with both fragments but two distinct groups of orbitals for the separate fragments. This sequence is often called ultrafast dissociation. The ultrafast dissociation was first observed for the HBr molecule after Br $3d$ excitation [23] and since then a number of investigations have been reported; only a few papers are cited here [24–29]. In this limiting case, the core-excited fragment is the F atom for the $1a_1 \rightarrow 6a_1$ promotion and CH_3 for the $2a_1 \rightarrow 6a_1$ promotion. The kinetic energy of the F atomic Auger line is known to be 656.5 eV for the $1s2p^6\ ^2S \rightarrow 2p^4\ ^1D$ transition [30]. Thus it should appear at a binding energy of ~ 31 eV in Fig. 1(a). The shadowed double-peak structure in Fig. 1(a) may indeed correspond to the F atomic Auger line that is split into two components due to the Doppler effect [24,26,28,29]. Hence a significant increase of the F^+ production in the binding energy interval 30–31 eV of the F $1s$ spectator Auger final states shown in Fig. 3 may be attributed to the ultrafast dissociation which exclusively produces F^+ . The corresponding significant increase of the CH^+ production in the binding energy interval

30–31 eV of the C $1s$ spectator Auger final states may be attributed to the ultrafast dissociation that produces the CH_n fragment with a $2a_1$ hole. In that case, the Auger decay occurs within the core-excited CH_n fragment and yields the CH^+ fragment via further breakup.

Through a close look at the electron spectrum in Fig. 1(a), however, one may notice that the energy of the F atomic Auger line is limited to the shadowed area and thus most of the electron emission may be attributed to molecular resonant Auger emission. The lifetime is ~ 3 fs for the $1a_1$ -hole state and the C–F elongation is limited to <0.4 Å in this time range [15,29]. Although the system undergoes resonant Auger decay mostly still in the molecular region, the elongation of the C–F distance proceeds within this time range and the Auger decay takes place outside the Franck-Condon region of photoabsorption. As the C–F bond elongates, the molecular orbitals start to be localized to either the C or the F site. The dominant F^+ production after the F KVV molecular emission suggests that the partial localization of the molecular orbitals already takes place. Following the same line of the argument, the enhancement of the CH^+ production after the C KVV emission is also considered to be a result of the molecular Auger emission taking place in this transient region. We note, however, that the C^+ and CH_2^+ yields are similar for the two site-selective excitations: only CH^+ varies. In order to understand this specific ion production, one needs theoretical study on potential surfaces of the relevant Auger final states and it is beyond the scope of the present experimental work.

Stolte *et al.* found a similar switching of the ion production in the anion-yield spectra of CH_3OH ; creation of the anionic OH^- fragment occurs only via resonant excitation below the C K edge [31]. They explained this site selectivity

as a result of two-hole localization of the carbon-containing fragment, which does not occur via the O $1s$ excitation. In this case the nuclear relaxation does not play any role. This contrasts with our finding on switching of the ion production, where the nuclear relaxation plays a key role in the charge localization.

V. CONCLUDING REMARK

The core excitation causes the C–F elongation in CH_3F . This nuclear relaxation transforms the molecular valence orbitals gradually into nonoverlapping valence orbitals of each fragment. The resonant Auger emission after F $1s$ or C $1s$ excitation takes place mostly in the transient region. As a result, the ion production, F^+ or CH^+ , is controlled by the location of the original core hole, $1a_1$ in the F site or $2a_1$ in the C site. We emphasize that the present observation provides the first clear evidence that the nuclear relaxation in the molecular core-excited state is responsible for switching the ion production via site-specific core excitation.

ACKNOWLEDGMENTS

The experiment was carried out with the approval of the SPring-8 program review committee and was partly supported by the Japan Society of the Promotion of Science (JSPS) in the form of Grants-in-Aid for Scientific Research. The staff of Spring-8 are greatly acknowledged for providing excellent experimental facility. E.K. is grateful to Tohoku University for hospitality and financial support during his stay in Japan. X.J.L. is grateful to Inoue Foundation and Tohoku University (COE Program) for financial support. C.M. is grateful to the JSPS for financial support.

-
- [1] K. Ueda and J. H. D. Eland, *J. Phys. B* **38**, S839 (2005).
 [2] W. Eberhardt, J. Stohr, J. Feldhaus, E. W. Plummer, and F. Sette, *Phys. Rev. Lett.* **51**, 2370 (1983).
 [3] W. Eberhardt, E. W. Plummer, I. W. Lyo, R. Carr, and W. K. Ford, *Phys. Rev. Lett.* **58**, 207 (1987).
 [4] D. M. Hanson, C. I. Ma, K. Lee, D. Lapieno-Smith, and D. Y. Kim, *J. Chem. Phys.* **93**, 9200 (1990).
 [5] K. Ueda, H. Chiba, Y. Sato, T. Hayaishi, E. Shigemasa, and A. Yagishita, *Phys. Rev. A* **46**, R5 (1992).
 [6] K. Ueda, K. Ohmori, M. Okunishi, H. Chiba, Y. Shimizu, Y. Sato, T. Hayaishi, E. Shigemasa, and A. Yagishita, *Phys. Rev. A* **52**, R1815 (1995).
 [7] C. Miron, M. Simon, N. Leclercq, D. L. Hansen, and P. Morin, *Phys. Rev. Lett.* **81**, 4104 (1998).
 [8] K. Ueda, M. Simon, C. Miron, N. Leclercq, R. Guillemin, P. Morin, and S. Tanaka, *Phys. Rev. Lett.* **83**, 3800 (1999).
 [9] P. Morin, M. Simon, C. Miron, N. Leclercq, E. Kukk, J. D. Bozek, and N. Berrah, *Phys. Rev. A* **61**, 050701(R) (2000).
 [10] K. Zähringer, H. D. Meyer, and L. S. Cederbaum, *Phys. Rev. A* **45**, 318 (1992).
 [11] T. X. Carroll, K. J. Borve, L. J. Sæthre, J. D. Bozek, E. Kukk, J. A. Hahne, and T. D. Thomas, *J. Chem. Phys.* **116**, 10221 (2002).
 [12] A. De Fanis, D. A. Mistrov, M. Kitajima, M. Hoshino, H. Shindo, T. Tanaka, H. Tanaka, Y. Tamenori, A. A. Pavlychev, and K. Ueda, *Phys. Rev. A* **71**, 052510 (2005).
 [13] G. Prümper, Y. Tamenori, A. De Fanis, U. Hergenbahn, M. Kitajima, M. Hoshino, H. Tanaka and K. Ueda, *J. Phys. B* **38**, 1 (2005).
 [14] G. Prümper, K. Ueda, U. Hergenbahn, A. De Fanis, Y. Tamenori, M. Kitajima, M. Hoshino, and H. Tanaka, *J. Electron Spectrosc. Relat. Phenom.* **144-147**, 227 (2005).
 [15] G. Prümper, K. Ueda, Y. Tamenori, M. Kitajima, N. Kuze, H. Tanaka, C. Makochekanwa, M. Hoshino, and M. Oura, *Phys. Rev. A* **71**, 052704 (2005).
 [16] H. Ohashi, E. Ishiguro, Y. Tamenori, H. Kishimoto, M. Tanaka, M. Irie, T. Tanaka, and T. Ishikawa, *Nucl. Instrum. Methods Phys. Res. A* **467-468**, 529 (2001).
 [17] H. Ohashi, E. Ishiguro, Y. Tamenori, H. Okumura, A. Hiraya, H. Yoshida, Y. Senba, K. Okada, N. Saito, I. H. Suzuki, K. Ueda, T. Ibuki, S. Nagaoka, I. Koyano, and T. Ishikawa, *Nucl. Instrum. Methods Phys. Res. A* **467-468**, 533 (2001).
 [18] T. Tanaka and H. Kitamura, *J. Synchrotron Radiat.* **3**, 47 (1996).

- [19] C. R. Brundle, M. B. Robin, and H. Basch, *J. Chem. Phys.* **53**, 2196 (1970).
- [20] L. Karlsson, R. Jadrny, L. Mattsson, F. T. Chau, and K. Siegbahn, *Phys. Scr.* **16**, 225 (1977).
- [21] G. Bieri, L. Asbrink, and W. Von Niessen, *J. Electron Spectrosc. Relat. Phenom.* **23**, 281 (1981).
- [22] C. M. Liegener, *Chem. Phys. Lett.* **151**, 83 (1988).
- [23] P. Morin and I. Nenner, *Phys. Rev. Lett.* **56**, 1913 (1986).
- [24] O. Björneholm, M. Bässler, A. Ausmees, I. Hjelte, R. Feifel, H. Wang, C. Miron, M. N. Piancastelli, S. Svensson, S. L. Sorensen, and F. Gel'mukhanov, and H. Ågren, *Phys. Rev. Lett.* **84**, 2826 (2000).
- [25] I. Hjelte, M. N. Piancastelli, R. F. Fink O. Björneholm, M. Bässler, R. Feifel, A. Giertz, H. Wang, K. Wiesner, A. Ausmees, C. Miron, S. L. Sorensen, and S. Svensson, *Chem. Phys. Lett.* **334**, 151 (2001).
- [26] K. Wiesner, A. Naves de Brito, S. L. Sorensen, F. Burmeister, M. Gisselbrecht, S. Svensson, and O. Björneholm, *Chem. Phys. Lett.* **354**, 382 (2002).
- [27] I. Hjelte, M. N. Piancastelli, C. M. Jansson, K. Wiesner, O. Björneholm, M. Bässler, S. L. Sorensen, and S. Svensson, *Chem. Phys. Lett.* **370**, 781 (2003).
- [28] K. Ueda, M. Kitajima, A. De Fanis, T. Furuta, H. Shindo, H. Tanaka, K. Okada, R. Feifel, S. L. Sorensen, H. Yoshida, and Y. Senba, *Phys. Rev. Lett.* **90**, 233006 (2003).
- [29] M. Kitajima, K. Ueda, A. De Fanis, T. Furuta, H. Shindo, H. Tanaka, K. Okada, R. Feifel, S. L. Sorensen, F. Gel'mukhanov, A. Baev, and H. Ågren, *Phys. Rev. Lett.* **91**, 213003 (2003).
- [30] S. Svensson, L. Larlsson, N. Mårtensson, P. Baltzer, and B. Wannberg, *J. Electron Spectrosc. Relat. Phenom.* **50**, C1 (1990).
- [31] W. C. Stolte, G. Öhrwall, M. M. Sant'Anna, I. Dominguez Lopez, L. T. D. Dang, M. N. Piancastelli, and D. W. Lindle, *J. Phys. B* **35**, L253 (2002).